NASA TECHNICAL MEMORANDUM

NASA TM X-52098

NASA TM X-52098

EFFECTS OF MOMENTUM BUFFER REGION ON COAXIAL FLOW OF DISSIMILAR FLUIDS

by Robert G. Ragsdale
Lewis Research Center
Cleveland, Ohio

TECHNICAL PREPRINT prepared for Propulsion Specialists Conference sponsored by the American Institute of Aeronautics and Astronautics Colorado Springs, Colorado, June 14-18, 1965

NATIONAL AERONAUTICS AND SPACE ADMINISTRATION · WASHINGTON, D.C. · 1965

E-2817

EFFECTS OF MOMENTUM BUFFER REGION ON COAXIAL FLOW OF DISSIMILAR FLUIDS

by Robert G. Ragsdale

Lewis Research Center
Cleveland, Ohio

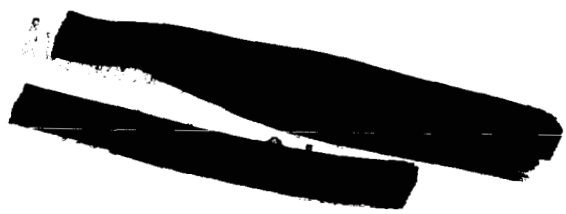

TECHNICAL PREPRINT prepared for
Propulsion Specialists Conference sponsored by the
American Institute of Aeronautics and Astronautics
Colorado Springs, Colorado, June 14-18, 1965

NATIONAL AERONAUTICS AND SPACE ADMINISTRATION

EFFECTS OF MOMENTUM BUFFER REGION ON COAXIAL FLOW OF DISSIMILAR FLUIDS

by Robert G. Ragsdale

Lewis Research Center
National Aeronautics and Space Administration
Cleveland, Ohio

ABSTRACT

18331

An analytical study was made of the isothermal mass and momentum transfer that occurs when a heavy, slow-moving gas is injected coaxially into a duct of light, fast-moving gas. The outer stream is composed of two regions; an outer region moving at high velocity, and an intermediate-velocity region adjacent to the inner fluid. As a basis for comparison, the total mass flow rate of outer fluid is held constant; thus as the buffer region velocity is decreased, the velocity of the remaining outer region is increased. The effects of the velocity and thickness of this buffer region on the mixing of the two fluids are investigated for both laminar and turbulent flow.

Outer- to inner-fluid initial-velocity ratios of 10, 50, and 100 are considered. Some representative velocity and concentration fields are shown for laminar and turbulent flow. The effect of a momentum buffer region is presented in terms of the amount of inner stream fluid that is contained within a specified length of the outer duct. The diameter of the duct is taken to be four times that of the jet; duct lengths of 2 and 4 jet diameters are considered.

In a gaseous-fueled nuclear rocket engine, stream mixing is undesirable because it tends to dilute the central care of fissionable gas with the surrounding hydrogen propellant, and thus leads to an increase in required reactor pressure. The results of this study show that both an "optimum" buffer velocity and thickness exist which give a maximum amount of inner fluid in the fixed length duct. The optimum velocity is greater for turbulent flow than for laminar flow. The optimum buffer thickness is shown to be independent of whether the flow is laminar or turbulent. For the system studied, the optimum buffer thickness is 1 inner stream radius. The presence of a

buffer region increases the amount of inner fluid in a duct length of 2 jet diameters by more than a factor of 2.

Author

INTRODUCTION

The interaction between two coaxially flowing fluids is a subject of considerable interest, both academic and practical. A description of mass, momentum, and energy transfer between dissimilar coaxial streams is required in order to understand and design combustion chambers, jet pumps and ejectors, and afterburners. Recent experimental and analytical studies have been reported that directly involve such a flow pattern. In a supersonic combustor,[1-4] a hydrogen jet is injected into a coflowing stream of oxidizer gas. In a proposed concept for a nuclear rocket engine,[5-7] a low-velocity, fissionable gas is injected into a coaxially flowing, high-velocity stream of hydrogen propellant. In both situations, the goal of the studies is to understand, to predict, and, ultimately, to control the mixing rate of the two species.

For the gaseous-fueled-reactor concept, the mixing is undesirable, because it tends to dilute the nuclear fuel with hydrogen and thus lead to an increase in required reactor pressure. Flow schemes that result in slower stream mixing are therefore of interest. Since the mixing occurs primarily because the outer stream velocity greatly exceeds that of the inner stream, it is possible, in principle, to delay the interaction of the two streams by separating them by means of a buffer region of fluid flowing at some intermediate velocity. This paper describes an analytical study of the characteristics of such a flow field.

In particular, the system to be considered is one in which a jet of low-velocity, heavy gas is separated from a surrounding, high-velocity, light gas by an annular sheath of intermediate-velocity, light gas. The gases are contained within a duct as illustrative n figure 1. The situation considered is one in which the total mass flow rate of the light gas is held constant as it might be in a rocket engine that is required to produce a certain amount of thrust. Thus as the velocity of the buffer region is reduced, the velocity of the remaining outer stream must be increased to maintain a constant mass flow rate.

The analytical method of reference 5 and its extension to turbulent flow[7] have been used to investigate the effects of a momentum buffer region on the coaxial mixing of dissimilar gases for isothermal flow. The primary parameters are the buffer region thickness and velocity. Calculations were carried out for both laminar and turbulent flow. Three values of average outer- to inner-stream-velocity ratio were considered. The results are compared with the case where no buffer region is present. The results presented indicate that a momentum buffer region can be used to alter significantly the rate of mixing in the near region of a coaxial jet.

NOMENCLATURE

b	width of mixing region, ft
c	concentration of inner stream species, mole fraction
$D_{1,1}$	molecular self-diffusion coefficient of species 1, ft^2/sec
$D_{1,2}$	binary diffusion coefficient of species 1 and 2, ft^2/sec
$\bar{D}$	dimensionless diffusion coefficient
K	a constant
M	molecular weight, lb/lb-mole
$Re_{1,0}$	initial Reynolds number of inner stream, $\frac{2r_{1,0}u_{1,0}\rho_{1,0}}{\mu_{1,0}}$
r	radial coordinate, ft
$\bar{r}$	dimensionless radius, $r/r_{1,0}$
$Sc_{1,0}$	initial Schmidt number of species 1, $\mu_{1,0}/\rho_{1,0}D_{1,1}$
$\bar{u}$	axial velocity, ft/sec
$\bar{v}$	molecular volume ratio
z	axial coordinate, ft
$\bar{z}$	dimensionless axial position, $z/r_{1,0}$
β	molecular weight parameter, $(M_1/M_2) - 1$
ϵ	eddy diffusivity, ft^2/sec
ϵ^+	dimensionless eddy viscosity, $\rho\epsilon/\mu$
η_b	normalized containment factor
η_c	containment factor

μ local viscosity

$\bar{\mu}$ dimensionless viscosity

ρ density, lb/ft^3

ψ stream function (see eqs. 5 and 6)

Subscripts:

av average

b buffer

max maximum

w wall

0 injection point ($z = 0$)

1 inner stream species

2 outer stream species

¢ centerline

ANALYTICAL METHOD

The basic analytical method used was reported in reference 5 for laminar flow and is extended to turbulent flow in references 6 and 7. It will be briefly reiterated here, along with a more detailed discussion of its application to a turbulent three-region system.

Laminar Flow

The steady-state boundary-layer equations for isothermal axisymmetric flow are:

Continuity:

$$\frac{\partial}{\partial r}(\rho v r) + \frac{\partial}{\partial z}(\rho u r) = 0 \tag{1}$$

Momentum:

$$v\frac{\partial u}{\partial r} + u\frac{\partial u}{\partial z} = \frac{1}{\rho r}\frac{\partial}{\partial r}\left(r\mu\frac{\partial u}{\partial r}\right) \tag{2}$$

Diffusion:

$$v\frac{\partial c}{\partial r} + u\frac{\partial c}{\partial z} = \frac{\rho}{r}\frac{\partial}{\partial r}\left(\frac{rD_{1,2}}{\rho}\frac{\partial c}{\partial r}\right) \tag{3}$$

The dimensional equations (1), (2), and (3) are made nondimensional by normalizing all

quantities to a dimensionally similar quantity in the inner stream at the injection point. For example, the dimensionless viscosity $\bar{\mu}$ is the ratio of local viscosity to that of pure inner stream fluid $\mu/\mu_{1,0}$; the axial velocity is normalized to the jet injection velocity so that $\bar{u} = u/u_{1,0}$; and the axial position and radius are normalized to the jet radius, $\bar{z} = z/r_{1,0}$ and $\bar{r} = r/r_{1,0}$. The dimensionless diffusion coefficient is given by $\bar{D} = (D_{1,2}/D_{1,1})$, where $D_{1,1}$ is the self-diffusion coefficient of the inner stream fluid.

The dimensionless continuity equation is now

$$\frac{\partial}{\partial \bar{r}}\left[\overline{rv}(\beta c + 1)\right] + \frac{\partial}{\partial \bar{z}}\left[\overline{ru}(\beta c + 1)\right] = 0 \tag{4}$$

where $\beta \equiv (M_1/M_2) - 1$. The system of equations is transformed from the $\bar{r}$, $\bar{z}$ plane to the ψ, $\bar{z}$ plane, where the stream function ψ satisfies the continuity equation (eq. (4)):

$$\frac{\partial \psi}{\partial \bar{z}} = -(\overline{rv})(\beta c + 1) \tag{5}$$

$$\frac{\partial \psi}{\partial \bar{r}} = (\overline{ru})(\beta c + 1) \tag{6}$$

By introducing dimensionless quantities and the stream function along with the usual boundary-layer assumption that $\partial\psi/\partial\bar{z} \ll d\psi/\partial\bar{r}$, equations (1), (2), and (3) can be written as follows:

Continuity:

$$\int_0^{\bar{r}} \bar{r}'\,d\bar{r}' = \int_0^{\psi} \frac{1}{\bar{u}(\beta c + 1)}\,d\psi' \tag{7}$$

Momentum:

$$\frac{\partial \bar{u}}{\partial \bar{z}} = 2\,\frac{\beta + 1}{Re_{1,0}}\,\frac{\partial}{\partial \psi}\left[\overline{\mu r^2}(\beta c + 1)\,\frac{\partial \bar{u}}{\partial \psi}\right] \tag{8}$$

Diffusion:

$$\frac{\partial c}{\partial \bar{z}} = \frac{2(\beta c + 1)}{Re_{1,0} Sc_{1,0}}\,\frac{\partial}{\partial \psi}\left[\overline{Dr^2}\,\frac{\partial c}{\partial \psi}\right] \tag{9}$$

The local viscosity is calculated from a mixing law that can be written in terms of dimensionless quantities as

$$\bar{\mu} = \frac{\beta c + 1}{(\beta + 1)c + \frac{1 - c}{\bar{\mu}_2}} \tag{10}$$

The dimensionless diffusion coefficient is obtained by writing the Gilliland equation (eq. (8)) in the form

$$\bar{D} \equiv \frac{D_{1,2}}{D_{1,1}} = \frac{2\sqrt{2(\beta + 2)}}{\left(1 + \bar{V}_2^{1/3}\right)^2} \tag{11}$$

where $\bar{V}_2$ is the ratio of molecular volumes of species 2 to species 1.

Equations (7) to (11) are solved numerically by computer program[5] to obtain radial profiles of dimensionless velocity and concentration at specified axial positions downstream from the injection point. In addition to constants relating to the numerical integration scheme, the following inputs are necessary and sufficient to define a case:

(1) Physical properties: β, $\bar{\mu}_2$, $\bar{V}_2$, $Sc_{1,0}$

(2) Flow parameter: $Re_{1,0}$

(3) Initial velocity profile: $\bar{u}(0,\bar{r})$

(4) Initial concentration profile: $c(0,\bar{r})$

For all the cases discussed in this paper, flat initial profiles are used, as illustrated in figure 1. For concentration, the initial profile is

$$0 \le \bar{r} \le 1 \qquad c = 1$$

$$1 < \bar{r} \le \bar{r}_{max} \qquad c = 0$$

With a buffer region, the initial velocity profile is

$$0 \le \bar{r} \le 1 \qquad \bar{u} = 1$$

$$1 < \bar{r} \le \bar{r}_b \qquad \bar{u} = \bar{u}_b$$

$$\bar{r}_b < \bar{r} \le \bar{r}_{max} \qquad \bar{u} = \bar{u}_{2,0}$$

and with no buffer region is

$$0 \le \bar{r} \le 1 \qquad \bar{u} = 1$$

$$1 < \bar{r} \le \bar{r}_{max} \qquad \bar{u} = \bar{u}_{2,0}$$

Turbulent Flow

The laminar analysis is extended to include turbulent flow by adding turbulent transport coefficients to their molecular counterparts. Thus the contribution of turbulence can be expressed in terms of a turbulent viscosity $\rho\epsilon$ and a turbulent diffusivity ϵ. It is also assumed that the eddy diffusivities for mass and momentum transfer are equal.

The transport properties in equations (2) and (3) are written as

$$\mu_t = \mu + \rho\epsilon \tag{12}$$

$$D_t = D + \epsilon \tag{13}$$

A similar procedure is employed in references 1 to 3, where it is further assumed that $\rho\epsilon \gg \mu$ and $\epsilon \gg D$.

Utilizing the same mixing law as for equation (10) gives a dimensionless total viscosity and diffusion coefficient in terms of a dimensionless eddy viscosity ϵ^+

$$\bar{\mu}_t = \frac{\beta c + 1}{\dfrac{(\beta + 1)c}{1 + \epsilon^+} \quad \dfrac{(1 - c)}{(1 + \epsilon^+)\bar{\mu}_2}} \tag{14}$$

$$\bar{D}_t = \frac{\beta c + 1}{\dfrac{(\beta + 1)c}{\bar{D} + \epsilon^+ Sc_{1,0}} + \dfrac{1 - c}{\bar{D} + \epsilon^+ \bar{\mu}_2 Sc_{1,0}(\beta + 1)}} \tag{15}$$

where

$$\epsilon^+ \equiv \frac{\rho\epsilon}{\mu}$$

The functional dependence of ϵ^+ remains to be specified in terms of spatial (r,z), flow (Re), and/or property (μ,ρ) characteristics of the system. This has been accomplished in current coaxial mixing studies by utilizing Prandtl's postulate that in a region of free turbulence the eddy diffusivity is proportional to the width of the mixing region and to the velocity difference across it:

$$\epsilon = Kb(u_{max} - u_{min}) \tag{16}$$

This postulate and its application to single-component jets and wakes are discussed in reference 9.

The extension of equation (16) to two-component systems can be achieved in

different ways. It has been suggested that $\rho\epsilon$ is constant with radius[1,2] and that the velocity difference should be replaced with $(\rho_2 u_2 - \rho_\ell u_\ell)$.[1] Reference 4 proposes that $\rho\epsilon$ is constant with radius and that a combination of mass flux ρu and momentum flux ρu^2 be employed. In reference 10 it is assumed that $\rho\epsilon/\mu$ is independent of radius, but dependent on axial position to some exponent. Reference 7 concludes that $\rho\epsilon/\mu$ can be taken as independent of radial and axial position and that the viscosity difference should be expressed as $(|u_2/u_1 - 1|)^{1/2}$.

Although these various approaches have yielded unresolved differences, they all share some significant similarities. All the suggested formulations (1) are in general agreement with experimental data, (2) are applicable for initial velocity ratios above and below 1, (3) indicate that the radial dependence of $\rho\epsilon$ is negligible, and (4) conclude that density ratio ρ_2/ρ_1 must be included as a parameter when applying equation (16) to two-component systems. These similarities suggest that each approximation will correlate data within certain ranges of flow and property parameters and that the difference between laminar and turbulent flow is much greater than the differences between the various algebraic descriptions of turbulent viscosity. The numerical solution of reference 5 and the turbulent viscosity expression of reference 7 have been used for the calculations reported herein because no linearization assumptions are required and because general agreement with turbulent coaxial mixing data has been demonstrated over the widest range of initial velocity ratios $(0.83 \leq \bar{u}_2 \leq 0.97,\ 1.25 \leq \bar{u}_2 \leq 49)$.

A recent study has shown that these various correlations predict about the sm turbulent viscosity at the jet origin when they are compared on a consistent basis. It is also shown that, for nearly equal stream velocities, turbulent mixing can be reduced by the presence of honeycomb inserts to remove "perturbulence" from the two streams just prior to the jet origin. The turbulent viscosity correlation of reference 7 used here included both the perturbulence and that due to the shear between the two free streams.

From reference 7, the ratio of turbulent to laminar viscosity can be written as

$$\epsilon^+ \equiv \frac{\rho\epsilon}{\mu} = 0.12\left(\frac{\mu_1}{\mu_2}\right)\left(\frac{M_2}{M_1}\right)(\mathrm{Re}_{1,0} - 250)(\bar{u}_2 - 1)^{1/2} \tag{17}$$

For a two-region coaxial-flow situation, u_2 is simply the initial velocity ratio of the outer to the inner fluid, and the use of equation (17) is straightforward. When a momentum buffer is present, there are two velocities in the outer fluid, and it is not so clear how to obtain one velocity to represent all of the outer fluid. Certainly this velocity should be some kind of average of the buffer region velocity and the outer region velocity, but there are a number of possibilities: a simple numerical average, a mass-flow-rate-weighted average, and a momentum-weighted average. The latter two procedures seem more realistic than a numerical average. For the most extreme case considered, the buffer region contained only 10 percent of total mass flow of the outer fluid, and 4 percent of the total momentum. Thus either of the two weighted averaging methods produced a velocity that was essentially the same as that of the high-velocity outer region. The choice, then, is rather academic; the $\bar{u}_2$ in equation (17) was evaluated with a momentum-weighted average velocity of the outer fluid.

SCHEDULE OF CALCULATIONS

The primary variables to be considered are the thickness of the buffer region, the velocity in the buffer region, and the initial velocity ratio of light gas to heavy gas. All calculations were made for both laminar and turbulent flow.

The first of each series of cases was for no buffer region present. For example, an initial velocity ratio of 10 was selected for the first case. For the next case, a buffer region thickness of 0.5 initial inner stream radii ($\bar{r}_b = 1.5$) was assigned, and the velocity ratio in this region was decreased until it was some specified fraction of that of the remaining outer fluid. A dimensionless channel radius $\bar{r}_w$ of 4 was assigned for all calculations, and as the buffer velocity was decreased, the velocity of the remaining outer fluid was increased to maintain a constant total mass flow rate of light gas. Thus if the initial velocity ratio with no buffer region is $\bar{\bar{u}}_{2,0}$, then

$$\bar{\bar{u}}_{2,0}(\bar{r}_w^2 - 1) = \bar{u}_b(\bar{r}_b^2 - 1) + \bar{u}_{2,0}(\bar{r}_w^2 - \bar{r}_b^2) \tag{18}$$

For the illustrative case selected, $\bar{\bar{u}}_{2,0} = 10$ and $\bar{r}_b = 1.5$; for a buffer velocity that is 0.1 of the remaining outer fluid velocity,

$$\bar{u}_{2,0} = \frac{\bar{\bar{u}}_{2,0}(\bar{r}_w^2 - 1)}{\left(\frac{\bar{u}_b}{\bar{\bar{u}}_{2,0}}\right)\left(\bar{r}_b^2 - 1\right) + \left(\bar{r}_w^2 - \bar{r}_b^2\right)} = 10.8$$

and $\bar{u}_b = 1.08$.

Average outer- to inner-velocity ratios of 10, 50, and 100 were considered. For each of these ratios, buffer- to outer-velocity ratios of 0.1, 0.2, 0.3, and 0.4 were investigated. For all combinations of these variables, buffer thicknesses of 0.5 and 1 were calculated, as well as the situation of no buffer region. These combinations were calculated for both laminar and turbulent flow:

Average outer- to inner-velocity ratio, $\bar{\bar{u}}_{2,0}$, 10, 50, 100

Buffer- to outer-velocity ratio, $\bar{u}_b/\bar{u}_{2,0}$, 0.1, 0.2, 0.3, 0.4

Buffer region radius, $\bar{r}_b$, 1, 15., 2.0

Flow regime, laminar, turbulent

For all calculations, the following constant values were used: $\beta = 100$, $\bar{\mu}_2 = 0.2$, $\bar{V}_2 = 0.2$, $Sc_{1,0} = 1.0$. As pointed out in references 5 and 10, the analytical results are relatively insensitive to the physical-property ratios, so these choices are not critical. Some of the calculations performed for this study were repeated for molecular Schmidt numbers of 0.5 and 2, and the concentration and velocity profiles were virtually unaffected. Insensitivity of a similar analysis to Schmidt number was reported in reference 4. The laminar calculations are based on an inner stream Reynolds number of 200 and the turbulent cases for a Reynolds number of 20 000.

RESULTS AND DISCUSSION

The results of the calculations of three-region, two-component mixing will be presented in two main categories. First, detailed characteristics of concentration and velocity fields will be discussed for both laminar and turbulent flow. Next, a more generalized presentation of the effects of a buffer region will be made in terms

of the total mass of inner stream fluid present in a channel of specified length.

Flow Field Characteristics

The general effect of a faster moving outer stream is to accelerate and dilute the inner stream fluid. This results from mass diffusion of the inner fluid radially outward into regions of higher velocity, and also from acceleration of the inner fluid by momentum transfer radially inward. Figure 2(a) shows the concentration field for turbulent coaxial flow with an initial velocity ratio of 50. If the initial velocity ratio were lower than 50, the mixing of the two streams would occur more slowly. A buffer region of lower velocity immediately adjacent to the inner stream presents such a situation, at least initially.

Figure 2(b) shows the effect of reducing the velocity in a buffer region, 1 jet radius in thickness, until it is 0.1 that of the remaining outer stream. In order to maintain the same mass flow of outer fluid, or the same average velocity ratio of 50, the outer-fluid-velocity ratio between the buffer region and the channel $\bar{r}_w = 4$ is increased to 61 and the buffer velocity ratio is 6.1. Figure 2(b) illustrates that the general effect of a momentum buffer is to reduce the mixing rate in the near region of the jet. Farther downstream, the mixing zone produced by the shear between the high velocity outer hydrogen flow and slow moving buffer region penetrates to the inner zone and results in increased acceleration of the inner fluid.

Figure 2(c) shows the concentration field that results if the buffer-to outer-velocity ratio is increased from 0.1 to 0.3. Although the buffer velocity is higher, the mixing rate is less than for a buffer-velocity ratio of 0.1. This indicates that there is an optimum buffer velocity and that buffer velocities below this value do not afford sufficient momentum in the buffer to offset the increased momentum in the outer stream required to maintain a constant mass flow. A comparison of the concentration lines $c = 0.6$ in figures 2(a) to (c) shows this effect. Figure 3 is a plot of centerline concentration as a function of axial position for the three cases first discussed. The centerline concentration is higher for a buffer-velocity ratio of 0.1 for only 1/2 jet radius downstream; beyond 2 radii downstream it falls below that for

no buffer region. Between axial distances of 1 and 4.5 jet radii, a buffer-velocity ratio of 0.3 affords more protection of the inner stream. Figure 3 also serves to illustrate that, although centerline concentrations exhibit an effect of a buffer, it is rather minimal. The effect of a buffer region on the velocity field is quite pronounced. This is shown in figure 4, again for turbulent flow and an average outer- to inner-velocity ratio of 50. Figure 4(a) is for no buffer region, and figure 4(b) is for a buffer thickness of 1 jet radius at a buffer- to outer-velocity ratio of 0.3. The reduction in the rate at which the inner fluid is accelerated is clearly shown by a comparison of the constant velocity lines for $\bar{u} = 5$ (fig. 4). The constant velocity lines for $\bar{u} = 49$ show that, farther downstream, the higher velocity outer fluid is beginning to overcome the initial buffer effect.

Figure 4 shows the entire velocity field regardless of species and does not threfore clearly reflect what has happened to the inner stream fluid. Figure 5 shows axial variation of the radially averaged velocity of the inner fluid, still for turbuleng flow, a buffer thickness of 1 jet radius, and an average initial velocity ratio of 50. The effect of a buffer region is shown more clearly in figure 5 than the centerline concentrations showed in figure 3. A buffer- to outer-velocity ratio of 0.3 has reduced the rate of acceleration of the inner stream fluid. At a distance of 8 jet radii downstream, the presence of a buffer with a velocity ratio of 0.1 has resulted in a higher velocity inner fluid than the case with no buffer region.

The influence of a buffer region on the average inner fluid velocity can be interpreted as an effect on the mean residence time of the inner fluid in a given length of channel. Thus the effect of a buffer region can be expressed in terms of its effect on the total mass of inner fluid that is contained in a channel of length $\bar{z}$, compared with the maximum amount that could be present. This maximum would occur for slip flow and no radial diffusion. The ratio of the total amount of inner fluid present to that which would exist with no interaction between the two streams is then a sort of "containment efficiency", or containment factor. It represents the degree to which the inner stream fluid has been swept from the system. It can vary from a maximum of 1.0 down to

$1/\bar{\bar{u}}_{2,0}$, which would represent instantaneous acceleration of the inner stream fluid.

Figure 6 shows a plot of this containment factor η_c for various channel lengths $\bar{z}$, turbulent flow, a buffer thickness of 1 jet radius, and $\bar{\bar{u}}/_{2,0} = 50$. Figure 6 shows the significant effect of a buffer region on the amount of inner stream fluid contained in a channel of length $\bar{z}$. For a system that is 4 jet radii in length, a buffer region with a buffer- to outer-velocity ratio of 0.3 increases the amount of inner fluid present from 18 percent without a buffer to 31 percent of the theoretical maximum. A buffer-velocity ratio of 0.1 yields a containment factor of 0.26.

Figures 7 and 8 show turbulent concentration fields for initial velocity ratios of 10 and 100, respectively. Comparison of these figures with figure 2 (for $\bar{\bar{u}}_{2,0} = 50$) indicates that the effect of a momentum buffer is more pronounced at higher initial velocity ratios, quantatively shown in succeeding figures.

For an initial velocity ratio of 50, the ratio of turbulent to laminar viscosity is 830 with no buffer region; this value was used in the calculation illustrated in figure 2(a). With a buffer region present, a momentum-averaged velocity of the outer fluid yields a value of 917 for $\rho\epsilon/\mu$ for the case shown in figure 2(b). Figures 9(a) and (b) show the corresponding concentration fields for laminar flow ($\rho\epsilon/\mu = 0$) for these two cases. A comparison of the concentration lines for $c = 0.2$ in figures 9(a) and (b) shows that a momentum buffer has a considerable effect for laminar flow, even though the general nature of the flow fields for laminar and turbulent mixing is markedly different.

Effect of Buffer Parameters on Containment Factors

Containment factors for laminar and turbulent flow are shown in figure 10 for basic coaxial mixing, with no buffer region present, and for initial velocity ratios of 10, 50, and 100. As before, the containment factor is the ratio of the total mass of jet fluid contained in a duct of length $\bar{z}$ to the amount that would be present with no interaction between the two streams. This containment factor serves as a measure of the degree of stream mixing. Higher initial velocity ratios, longer ducts, or the presence of turbulence all lead to increased mixing and lower containment factors.

The presence of a momentum buffer region reduces stream mixing and increases the

containment factor. The effects of buffer-region thicknesses and velocities on the containment factor are shown in figure 11 for laminar flow and in figure 12 for turbulent flow. Curves are shown for buffer-region thicknesses of 0.5 and 1.0 jet radii and for initial average velocity ratios of 10, 50, and 100.

The curves exhibit the same general effect of buffer velocity on containment factor for laminar and turbulent flow. As the buffer-region velocity is decreased, the containment factor increases to a maximum value and then begins to decrease. A comparison of two corresponding curves for $\bar{z}$ values of 4 and 8 shows that the buffer effect is reduced for longer ducts, but that the optimum buffer- to outer-velocity ratio is essentially the same. The remaining results will be presented for a duct that is 4 jet radii in length ($\bar{z} = 4$).

It is difficult to assess the relative effects of a buffer region from the various curves of figures 11 and 12 because the absolute value of the containment factor is strongly affected by the initial velocity ratio and by the nature of the flow. It is therefore useful to normalize each curve to its value with no buffer region ($\bar{u}_b/\bar{u}_{2,0} = 1.0$).

The variation of such a normalized containment factor η_b with buffer- to outer-velocity ratio is shown in figure 13. The parameter η_b is the factor by which the amount of jet fluid in the duct has been increased by a buffer region. For an average velocity ratio of 100, a buffer that is 1 jet radius thick ($\bar{r}_b = 2$) and for turbulent flow, the amount of jet fluid in the duct is increased by a factor of 2.25 by decreasing the buffer-velocity ratio $\bar{u}_b/\bar{u}_{2,0}$ from 1 (no buffer) down to 0.2. The maximum buffer effect is obtained for a buffer-velocity ratio of approximately 0.2, though there is some variation. Figure 14 shows the optimum buffer-velocity ratio as a function of the average initial velocity ratio $\bar{\bar{u}}_{2,0}$. For higher initial velocity ratios, the optimum buffer-velocity ratio is lower. In general, the optimum buffer velocities range from 0.2 to 0.4 of the outer velocity for turbulent flow and from 0.1 to 0.3 for laminar flow. Thicker buffer regions require lower buffer velocities.

Figure 15 shows the effect of the thickness of the buffer region on containment

factors that have been maximized with respect to the buffer-velocity ratio. As with buffer-velocity ratio, an optimum exists. Higher initial average velocity ratios require somewhat thickner buffer regions, but the effect is relatively weak. For the range of conditions studied, the optimum momentum buffer thickness is approximately 1 jet radius. It is interesting to note that the optimum buffer thickness is virtually independent of whether the flow is laminar or turbulent.

CONCLUSIONS

The results of this study indicate some characteristics of two-component, three-region coaxial flow. All the calculations were carried out for a channel- to jet-radius ratio of 4, and for the following physical properties: A ratio of inner fluid to outer fluid molecular weight a ratio of 100, an inner fluid Schmidt number of 1, a ratio of outer-fluid to inner-fluid viscosity of 0.2, and a ratio of outer-fluid to inner-fluid molecular volume of 0.2. For laminar-flow calculations, the jet Reynolds number was taken as 200; for turbulent flow, the jet Reynolds number was taken to be 20 000. Channel lengths of 4 and 8 jet radii were considered, and buffer thicknesses of 0, 0.5, and 1 jet radii were investigated. Average ratios of outer-fluid to inner-fluid initial velocity of 10, 50, and 100 were studied; for each of these cases, buffer- to outer-initial velocity ratios of 0.1, 0.2, 0.3, and 0.4 were considered. For these ranges of conditions, the following results were obtained:

1. An optimum buffer-region velocity exists that minimizes the interaction between the two fluids.

2. Similarly, there is an optimum buffer-region thickness.

3. The optimum buffer velocities range from 0.2 to 0.4 of the outer velocity for turbulent flow and from 0.1 to 0.3 for laminar flow.

4. The effect of a momentum buffer region is greater for higher initial velocity ratios of outer stream to inner stream fluid.

5. For a duct radius that is four times that of the jet, the optimum buffer thickness is 1 jet radius for both laminar and turbulent flow.

6. The presence of an intermediate-velocity momentum-buffer region of outer fluid

significantly affects mass and momentum transfer and can increase the amount of inner fluid contained in a duct 4 jet radii in length by more than a factor of 2.

REFERENCES

1. Libby, P. A.: Theoretical Analysis of Turbulent Mixing of Reactive Gases With Application to Supersonic Combustion of Hydrogen. ARS J., 388-396, Mar. 1962.
2. Ferri, A., Libby, P. A., and Zakkay, V.: Theoretical and Experimental Investigation of Supersonic Combustion. High Temperatures in Aeronautics, pp. 55-118, Pergamon Press, New York, 1964.
3. Zakkay, V., Krause, E., and Woo, S. D. L.: Turbulent Transport Properties for Axisymmetric Heterogeneous Mixing. PIBAL Rpt. No. 813, Mar. 1964.
4. Alpinieri, L. J.: Turbulent Mixing of Coaxial Jets. AIAA J., 1560-1567, Sept. 1964.
5. Weinstein, H., and Todd, C. A.: A Numerical Solution of the Problem of Mixing of Laminar Coaxial Streams of Greatly Different Densities - Isothermal Case. NASA TN D-1534, Feb. 1963.
6. Ragsdale, R. G., and Weinstein, H.: On the Hydrodynamics of a Coaxial Flow Gaseous Reactor. Proceedings of Nuclear Propulsion Conference, AEC TID-7653, Pt. 1, pp. 82-88, July 1963.
7. Ragsdale, R. G., Weinstein, H., and Lanzo, C. D.: Correlation of a Turbulent Air-Bromine Coaxial-Flow Experiment. NASA TN D-2121, Feb. 1964.
8. Sherwood, T. K.: Absorption and Extraction. McGraw-Hill Book Co., Inc., 1937, p.18.
9. Schlichting, H.: Boundary Layer Theory. Fourth Ed., McGraw-Hill Book Co., Inc., 1960, Chapters XIX and XXIII.
10. Weinstein, H., and Todd, C. A.: Analysis of Mixing of Coaxial Streams of Dissimilar Fluids Including Energy-Generation Terms. NASA TN D-2123, March 1964.
11. Ragsdale, R. G., and Edwards, D. J.: Turbulent Coaxial Mixing of Dissimilar Gases at Nearly Equal Stream Velocities. NASA TM X-52082, Feb. 1965.

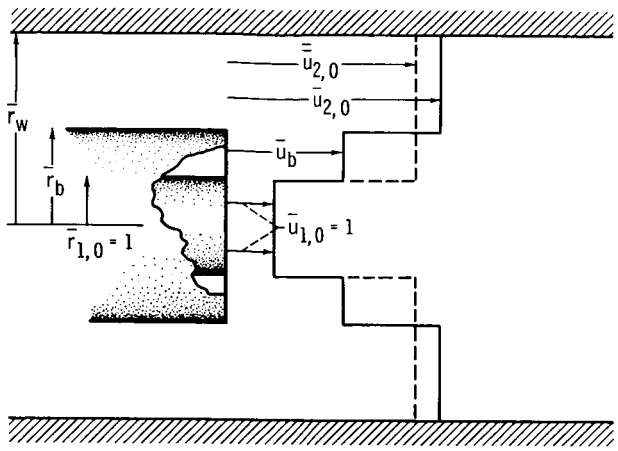

Figure 1. - Calculation model.

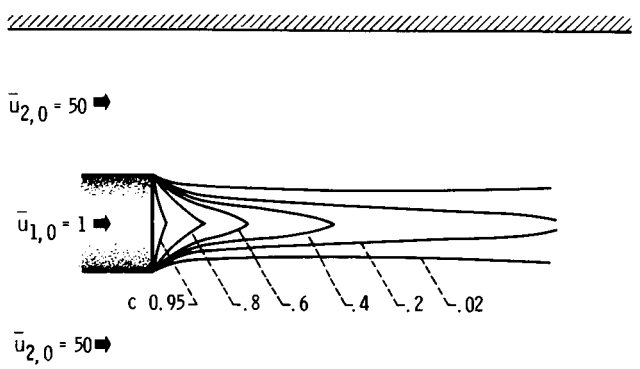

(a) No buffer region.

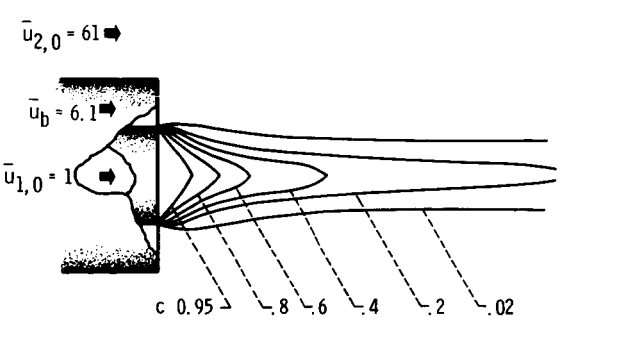

(b) Buffer thickness, 1; $\bar{u}_b/\bar{u}_{2,0} = 0.1$.

Figure 2. - Effect of buffer region on concentration field. Turbulent flow; $\bar{u}_{2,0} = 50$.

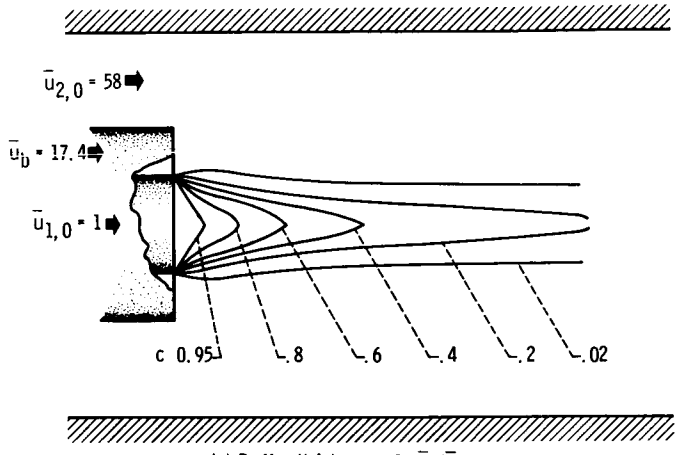

(c) Buffer thickness, 1; $\bar{u}_b/\bar{u}_{2,0}$ = 0.3.

Figure 2. - Concluded.

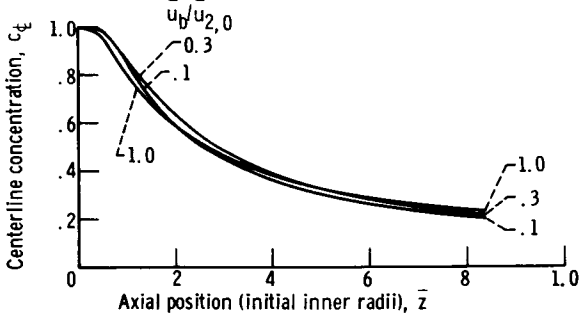

Figure 3. - Centerline concentration. Turbulent flow; $\bar{u}_{2,0}$ = 50; buffer thickness, 1.

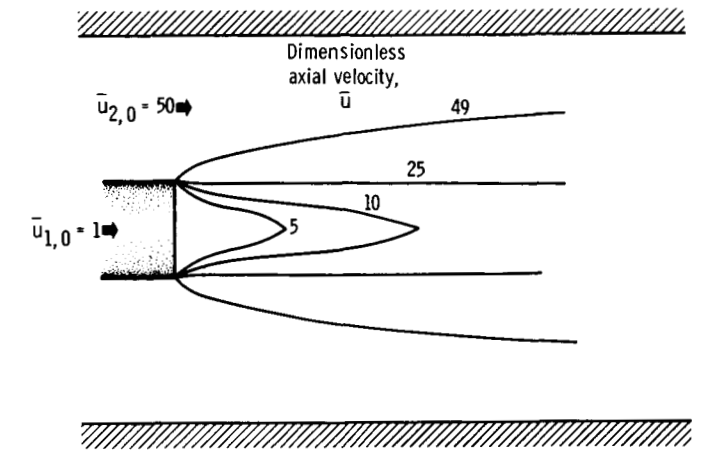

(a) No buffer region.

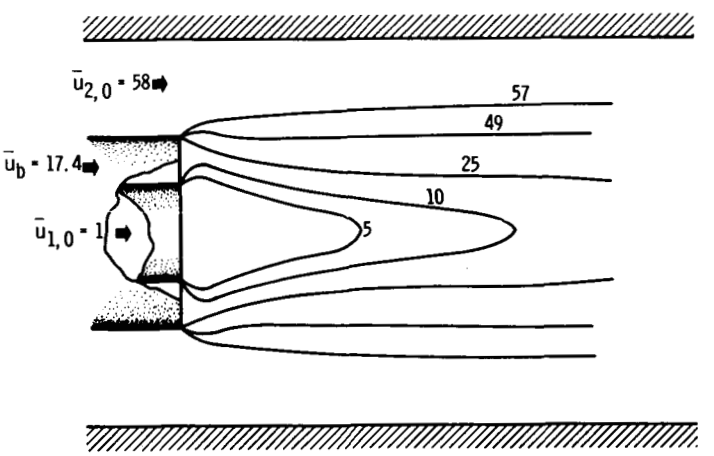

(b) Buffer thickness, 1; $\bar{u}_b/\bar{u}_{2,0}$ = 0.3.

Figure 4. - Effect of buffer region on velocity field. Turbulent flow; $\bar{u}_{2,0}$ = 50.

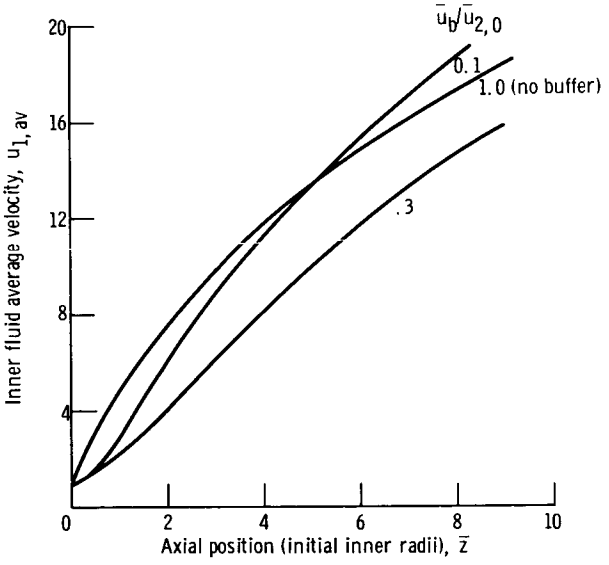

Figure 5. - Effect of buffer region on inner fluid average velocity. Turbulent flow; $\bar{u}_{2,0} = 50$; buffer thickness, 1.

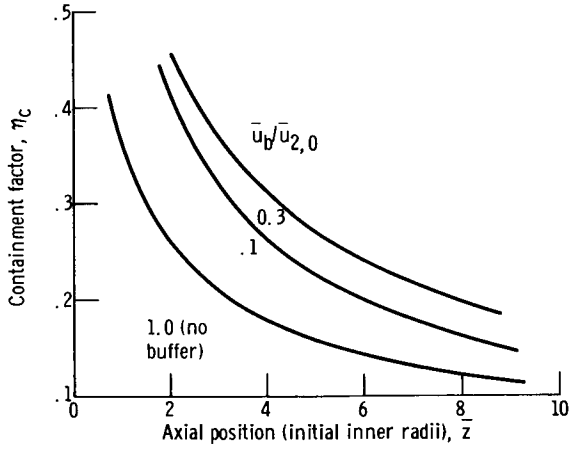

Figure 6. - Effect of buffer region on total mass of inner fluid in system of length z. Turbulent flow; $\bar{u}_{2,0} = 50$; buffer thickness, 1.

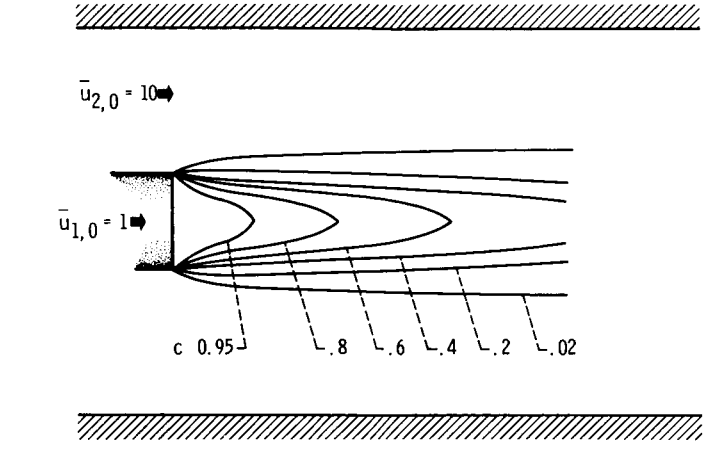

(a) No buffer.

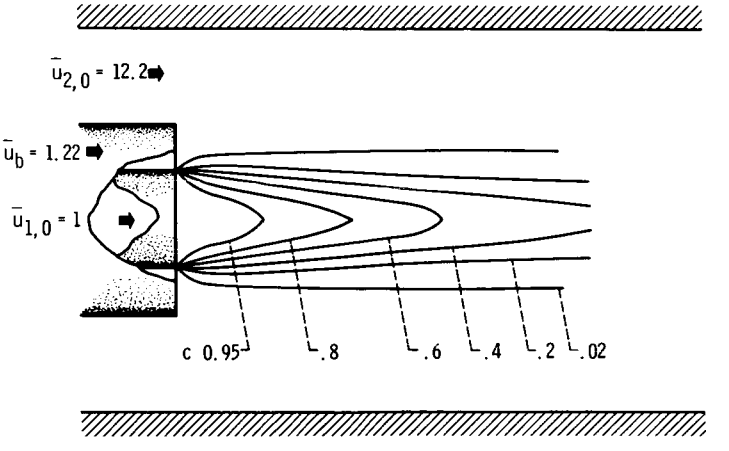

(b) Buffer thickness, l; $\bar{u}_b/\bar{u}_{2,0} = 0.1$.

Figure 7. - Effect of buffer region on concentration field. Turbulent flow; $\bar{u}_{2,0} = 10$.

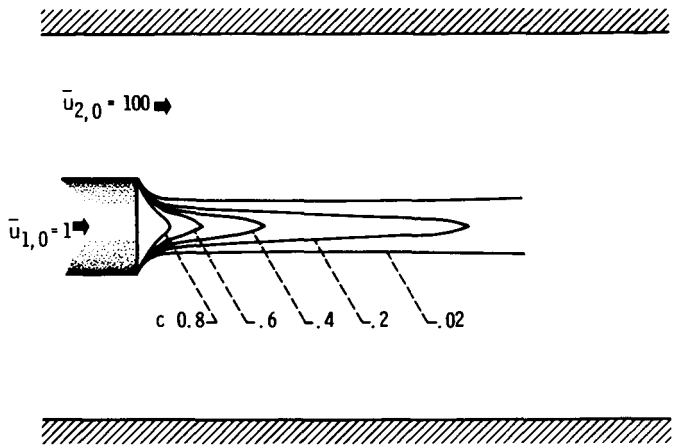

(a) No buffer.

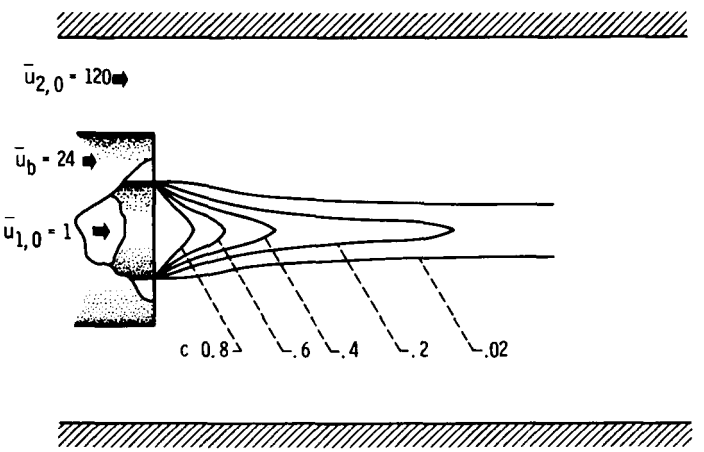

(b) Buffer thickness, 1; $\bar{u}_b/\bar{u}_{2,0}$ = 0.2.

Figure 8. - Effect of buffer region. Turbulent flow; $\bar{u}_{2,0}$ = 100.

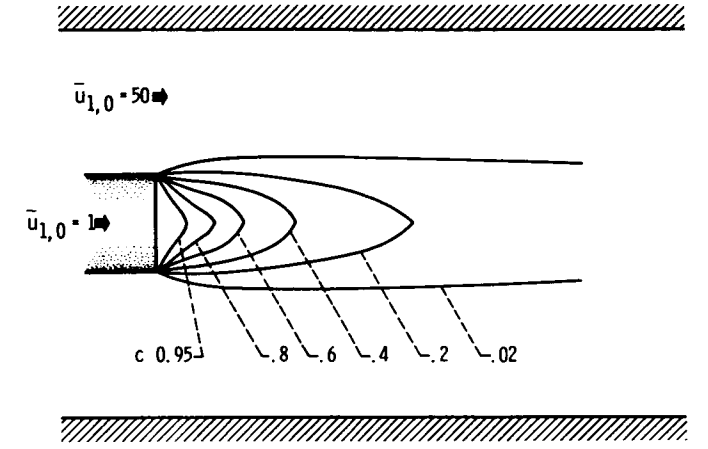

(a) No buffer region.

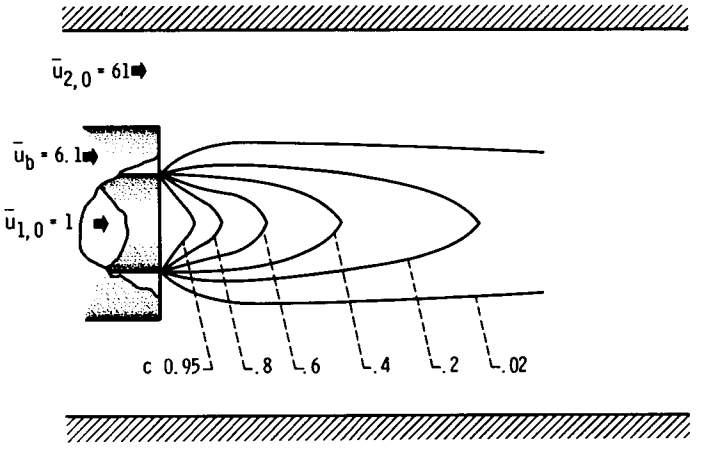

(b) Buffer thickness, l; $\bar{u}_b/\bar{u}_{2,0}$ = 0.1.

Figure 9. - Effect of buffer region on concentration field. Laminar flow; $\bar{\bar{u}}_{2,0}$ = 50.

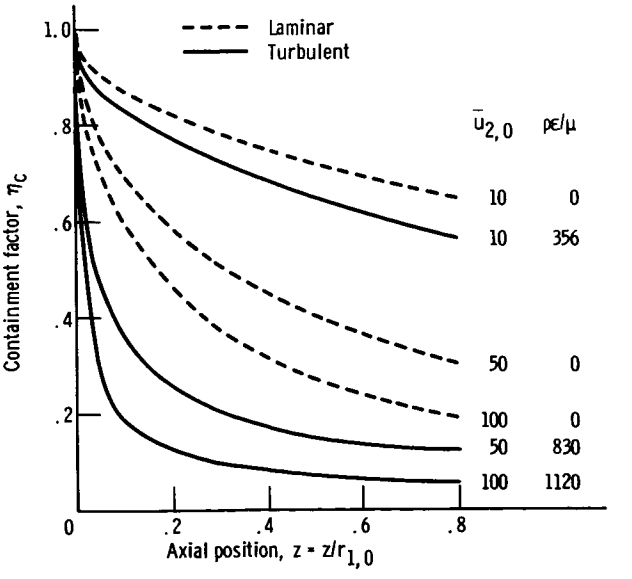

Figure 10. - Containment factors. No buffer region.

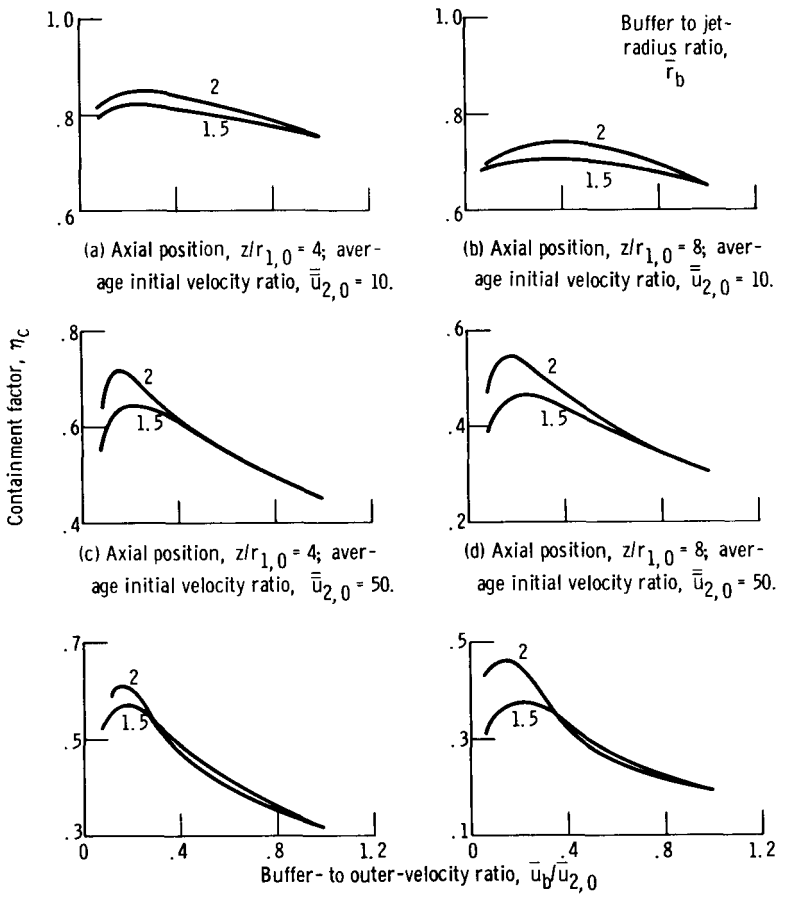

(a) Axial position, $z/r_{1,0} = 4$; average initial velocity ratio, $\bar{\bar{u}}_{2,0} = 10$.

(b) Axial position, $z/r_{1,0} = 8$; average initial velocity ratio, $\bar{\bar{u}}_{2,0} = 10$.

(c) Axial position, $z/r_{1,0} = 4$; average initial velocity ratio, $\bar{\bar{u}}_{2,0} = 50$.

(d) Axial position, $z/r_{1,0} = 8$; average initial velocity ratio, $\bar{\bar{u}}_{2,0} = 50$.

(e) Axial position, $z/r_{1,0} = 4$; average initial velocity ratio $\bar{\bar{u}}_{2,0} = 100$.

(f) Axial position, $z/r_{1,0} = 8$; average initial velocity ratio, $\bar{\bar{u}}_{2,0} = 100$.

Figure 11. - Buffer containment factors. Laminar flow.

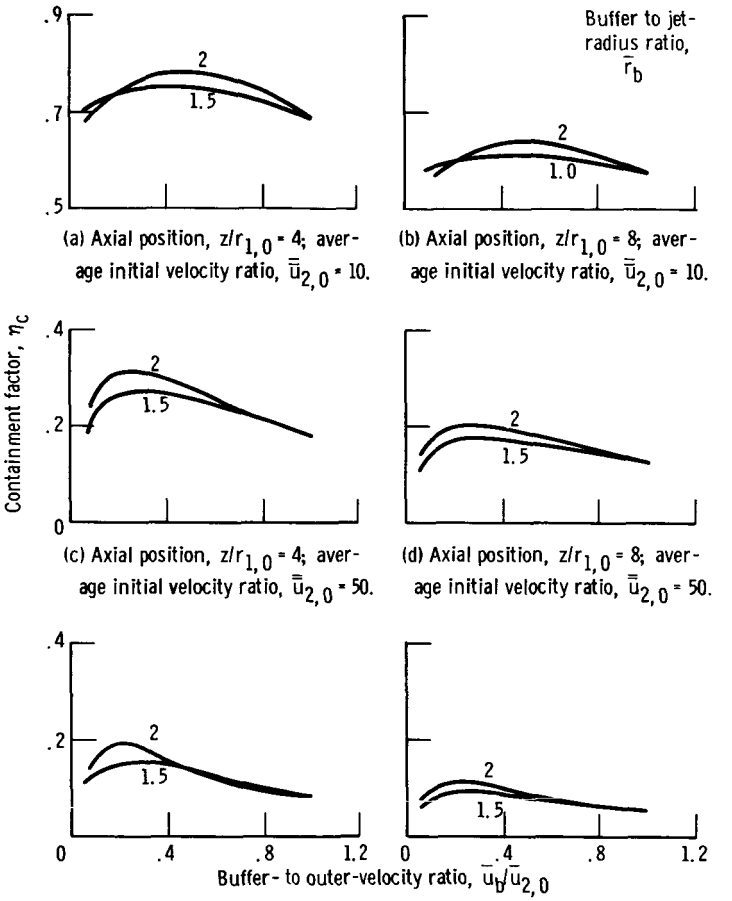

(a) Axial position, $z/r_{1,0} = 4$; average initial velocity ratio, $\bar{\bar{u}}_{2,0} = 10$.

(b) Axial position, $z/r_{1,0} = 8$; average initial velocity ratio, $\bar{\bar{u}}_{2,0} = 10$.

(c) Axial position, $z/r_{1,0} = 4$; average initial velocity ratio, $\bar{\bar{u}}_{2,0} = 50$.

(d) Axial position, $z/r_{1,0} = 8$; average initial velocity ratio, $\bar{\bar{u}}_{2,0} = 50$.

(e) Axial position, $z/r_{1,0} = 4$; average initial velocity ratio, $\bar{\bar{u}}_{2,0} = 100$.

(f) Axial position, $z/r_{1,0} = 8$; average initial velocity ratio, $\bar{\bar{u}}_{2,0} = 100$.

Figure 12. - Buffer containment factors. Turbulent flow.

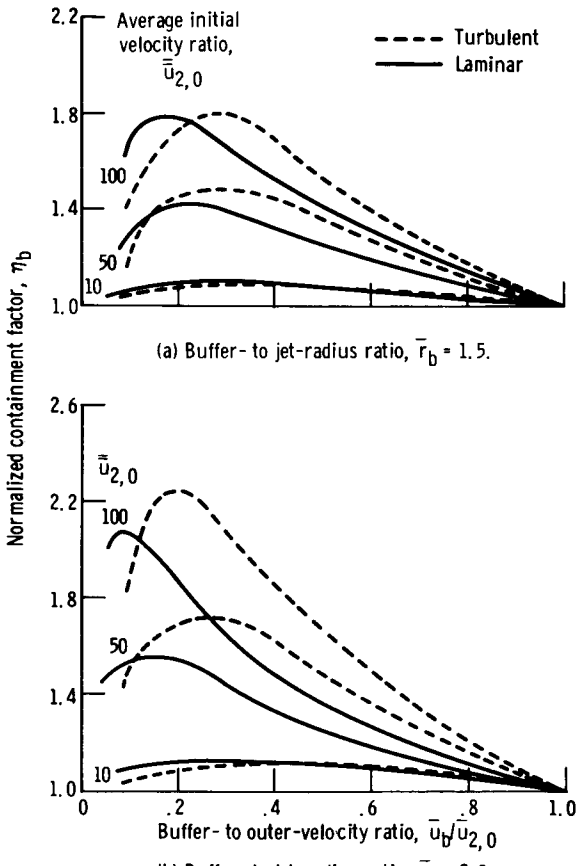

Figure 13. - Normalized buffer containment factors for $z/r_{1,0} = 4$.

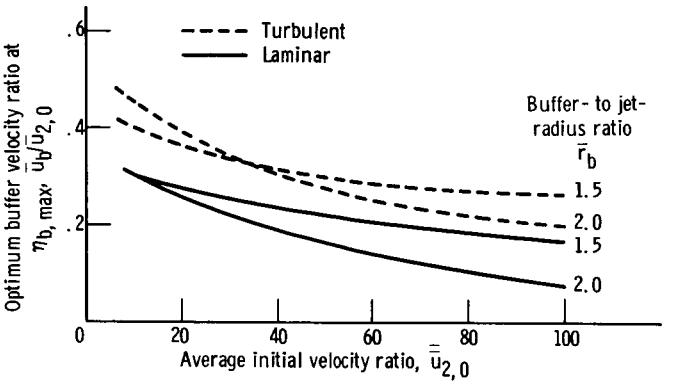

Figure 14. - Optimum-buffer to primary-velocity ratios for $z/r_{1,0} = 4$.

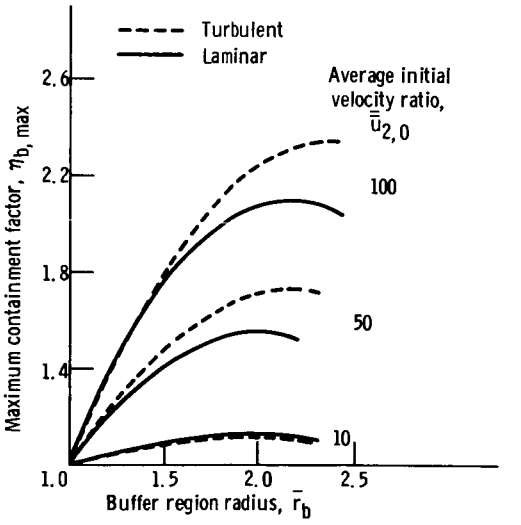

Figure 15. - Optimum buffer thicknesses for $z/r_{1,0} = 4$.